NCGIA

National Center for Geographic Information and Analysis

Two Papers on Triangulated Surface Modeling

by:

Carlos Felgueiras

Divisao de Processamento de Imagens (DPI)
Instituto Nacional de Pesquisas Espaciais (INPE)
Sfio Jose dos Campos, Sao Paulo, Brazil

and

Michael F. Goodchild

University of California, Santa Barbara

Technical Report 95-2

January 1995

Simonett Center for Spatial Analysis
University of California
35 10 Phelps Hall
Santa Barbara, CA 93106-4060
Office (805) 893-8224
Fax (805) 893-8617
ncgia@ncgia.ucsb.edu

State University of New York
301 Wilkeson Quad, Box 610023
Buffalo NY 14261-0001
Office (716) 645-2545
Fax (716) 645-5957
ncgia@ubvms.cc.buffalo.edu

University of Maine
348 Boardman Hall
Orono ME 04469-5711
Office (207) 581-2149
Fax (207) 581-2206
ncgia@spatial.maine.edu

Title:

A COMPARISON OF THREE TIN SURFACE MODELING METHODS AND ASSOCIATED ALGORITHMS

Authors and affiliations:

CARLOS A. FELGUEIRAS

Divisão de Processamento de Imagens (DPI), Instituto Nacional de Pesquisas Espaciais (INPE), São José dos Campos, São Paulo, Brazil.

MICHAEL F. GOODCHILD

National Center for Geographic Information and Analysis (NCGIA), Geography Department University of California Santa Barbara (UCSB), California, USA.

Keywords:

triangulation, interpolation, surface fitting, digital terrain model, fractal.

Short title:

A comparison of three TIN surface modeling methods.

Name and address of the author for correspondence:

Carlos A. Felgueiras

DPI - INPE (Instituto Nacional de Pesquisas Espaciais)

Av. dos Astronautas 1758 - Jardim da Granja - São José dos Campos - SP

CEP 12227 010 - C.P. 515 - São Paulo - Brasil

Fone: 011 55 123 418977 ext 372

Fax: 011 55 123 21 87 43

E-mail: carlos@dpi.inpe.br

Acknowledgments:

We want to express our gratitude to Uwe Deichmann and Julio C. L. D'Alge for helpful suggestions. We also would like to thank Jonathan Gottesegen and Darrel Lamb for their useful remarks and comments on earlier drafts of this paper. This work was performed while the first author was at the National Center for Geographic Information and Analysis (NCGIA) at the University of California Santa Barbara.

A comparison of three TIN surface modeling methods and associated algorithms

Abstract. This paper describes the implementation of three methods for fitting surfaces: linear, quintic and stochastic. It uses qualitative (visual) and quantitative (statistical) criteria to compare the three approaches. The digital terrain model is based on a triangular irregular network (TIN) structure and the comparison is performed using a mathematically defined function and real data obtained from a raster digital elevation model (DEM) from a United States Geological Survey (USGS) elevation file.

1. Introduction

Digital surface representation from a set of three-dimensional samples is an important issue of computer graphics that has applications in different areas of study such as engineering, geology, geography, meteorology, medicine, etc. The digital model allows important information to be stored and analyzed without the necessity of working directly with the real surface. In addition, we can integrate products from Digital Terrain Model (**DTM**) manipulation with other data in a Geographical Information System (**GIS**) environment. MacCullagh (1988) presents a detailed study of DTMs, considering their merge with image processing and database systems.

The main objective of this work is the comparison of different methodologies to model surfaces from a set of scattered three dimensional samples. The basic structure used to represent the surface is the *triangular irregular network,* whose triangle vertices are the sample points. Another goal of the work is the evaluation of the relative precision of digital models for representing spatial variation as exactly as possible.

This work presents three methods for triangular surface fitting: *linear, quintic* and *stochastic*. It also gives a qualitative (visual) and a quantitative (statistical) analysis of the three methods using both a mathematically defined function and digital elevation model data, hereafter called DEM-USGS, as supplied by the United States Geological Survey.

Section 2 introduces the basic concepts related to surface fitting for TIN model structures. Section 3 describes the methodology used to compare the surface fitting interpolators. Section 4 shows and analyzes the results achieved using the proposed methodology. Section 5 presents the conclusions and some suggestions for future research related to this work.

2. Triangular Irregular Networks

This work compares the accuracy of different algorithms to fit surfaces for TIN models. De Floriani (1992), Falcidieno (1993) and Tsai (1993) are recent contribuitions to the vast literature on the study and implementation of DTMs based on TIN structures. In this section we present only the principal characteristics of TIN models.

A TIN *represents a surface as a set of non-overlapping contiguous triangular facets, of irregular size and shape* (Chen 1987). TIN uses the data on the irregularly spaced samples as the basis of a system of triangulation (Burrough 1986). It is created directly from the set of samples, i. e. the vertices of the triangles are the samples. Commonly a TIN is constructed using the bidimensional projection of the sample points in the xy plane. When the sample set is too dense, it is necessary to apply an algorithm that chooses a subset, the *very important points* (**VIP**), that better represents the original surface. This approach reduces the number of points used to create the TIN model. Lee (1991) performs a comparison of 3 algorithms to reduce the number of points

to construct TIN models from rectangular grid DEMs. In some cases, as when the samples are contour lines, it is imperative to use algorithms for cartographic generalization.

The most popular TIN model, used in commercial software, is the Delaunay TIN. The Delaunay triangulation is the straight-line dual of the Voronoi diagram and is constructed by connecting the points whose associated Voronoi polygons share a common edge. The Delaunay TIN has the following properties:

- It is unique and;
- It maximizes the minimum internal angles of each triangle, i. e. the minimum angle of its triangles is maximum over all triangulations. This characteristic avoids the creation of thin triangles, i. e. each triangle is as equilateral as possible.

The circumference that passes through the three vertices of a Delaunay triangle does not contain any other sample point. This property is known as the *empty circle criterion* (Tsai 1993). This property is used to construct the TIN model directly from the sample set. Figure 1 illustrates the use of the empty circle criterion condition to determine whether a triangle is Delaunay or not.

Another interesting triangular model is the *greedy TIN*. This network is constructed with triangles that have the shortest possible edges. Greedy triangulation has been used to hasten the task to find the nearest neighborhood of a sample point. Preparata (1988) describes some methods to create greedy triangulations.

2.1. *Fitting surfaces for TIN models*

In this work we are interested in DTMs whose basic structures are triangular networks. Each basic element of the TIN, a triangle, can be described by a local polynomial surface whose parameters depend on its own vertices and, usually, on its triangular neighborhood. This section

will discuss three different approaches to interpolate TIN models: linear, quintic and stochastic triangular surface fitting.

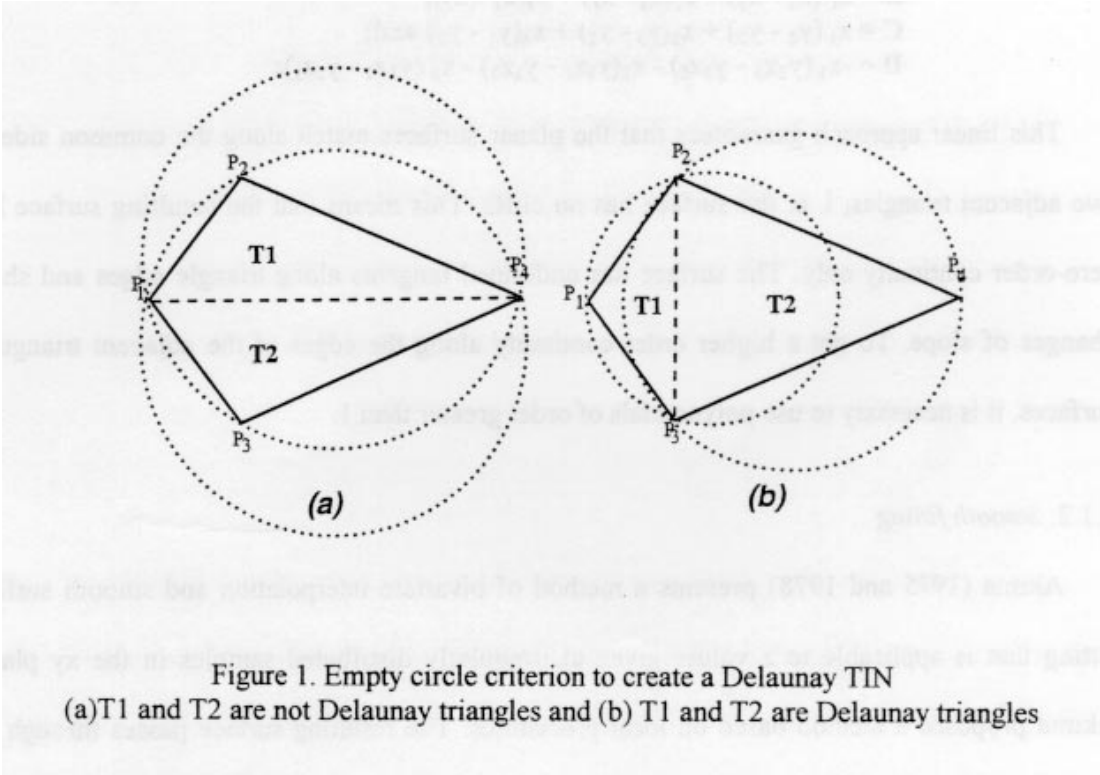

Figure 1. Empty circle criterion to create a Delaunay TIN
(a)T1 and T2 are not Delaunay triangles and (b) T1 and T2 are Delaunay triangles

2.1.1. *Linear fitting*

Each triangle of the TIN model defines a plane that is used to determine the z value of every point **(x, y)** inside the triangle. The equation of a plane surface can be expressed as:

$$\mathbf{Ax + By + Cz + D = 0;} \qquad \mathbf{(1)}$$

To calculate the coefficients **A, B, C** and **D** of the equation 1 it is enough to use the z value of the 3 vertices of the triangle. Suppose that the three vertices of the triangle have the coordinates: $\mathbf{(x_1, y_1, z_1)}$, $\mathbf{(x_2, y_2, z_2)}$ and $\mathbf{(x_3, y_3, z_3)}$. These three points define the following linear equation system:

$$\mathbf{(A/D)x_i + (B/D)y_i + (C/D)z_i = -1; \quad where\ i = 1,2,3} \qquad \mathbf{(2)}$$

The solution of this system, using Cramer's rule for example, gives:

$$\mathbf{A = y_1 (z_2 - z_3) + y_2(z_3 - z_1) + y_3(z_1 - z_2);} \quad \mathbf{(3)}$$

$$\mathbf{B = z_1 (x_2 - x_3) + z_2(x_3 - x_1) + z_3(x_1 - x_2);} \quad \mathbf{(4)}$$

$$\mathbf{C = x_1 (y_2 - y_3) + x_2(y_3 - y_1) + x_3(y_1 - y_2) \text{ and;}} \quad \mathbf{(5)}$$

$$\mathbf{D = -x_1 (y_2z_3 - y_3z_2) - x_2(y_3z_1 - y_1z_3) - x_3 (y_1z_2 - y_2z_1);} \quad \mathbf{(6)}$$

This linear approach guarantees that the planar surfaces match along the common side of two adjacent triangles, i. e. the surface has no cliffs. This means that the resulting surface has zero-order continuity only. The surface has undefined tangents along triangle edges and sharp changes of slope. To get a higher order continuity along the edges of the adjacent triangular surfaces, it is necessary to use polynomials of order greater than 1.

2.1.2. *Smooth fitting*

Akima (1975 and 1978) presents a method of bivariate interpolation and smooth surface fitting that is applicable to z values given at irregularly distributed samples in the xy plane. Akima proposed a method based on local procedures. The resulting surface passes through all the given samples and has continuity of order 2, i. e. slopes and curvatures change smoothly, even across triangle edges. In sum, it is an algorithm to smoothly fit surfaces over every basic element of a triangular mesh. A more detailed study of smoothness and derivatives can be found in Lancaster (1986).

Akima proposed to fit a quintic polynomial function for each triangle. He used the following fifth-degree polynomial in x and y to evaluate the function at any point **(x, y)** inside the triangle:

$$\mathbf{z(x, y) = \sum_{i=0}^{5} \sum_{j=0}^{5-i} q_{ij} x^i y^j} \quad \mathbf{(7)}$$

To determine the 21 coefficients $\mathbf{q_{ij}}$, in order to solve the equation 7, one has to use the information from the 3 vertex points **(p1= (x_1, y_1, z_1), p2=(x_2, y_2, z_2)** and **p3=(x_3, y_3, z_3))** of the triangle and their neighbors. For these vertices one must obtain:

- The z values of the vertex points:

$$\mathbf{z_1, z_2 \text{ and } z_3;}$$

- The first order partial derivatives:

$$\left.\frac{\partial z}{\partial x}\right|_{p=p1}, \left.\frac{\partial z}{\partial x}\right|_{p=p2}, \left.\frac{\partial z}{\partial x}\right|_{p=p3}, \left.\frac{\partial z}{\partial y}\right|_{p=p1}, \left.\frac{\partial z}{\partial y}\right|_{p=p2} \text{ and } \left.\frac{\partial z}{\partial y}\right|_{p=p3};$$

- The second order partial derivatives:

$$\left.\frac{\partial^2 z}{\partial x^2}\right|_{p=p1}, \left.\frac{\partial^2 z}{\partial x^2}\right|_{p=p2}, \left.\frac{\partial^2 z}{\partial x^2}\right|_{p=p3}, \left.\frac{\partial^2 z}{\partial y^2}\right|_{p=p1}, \left.\frac{\partial^2 z}{\partial y^2}\right|_{p=p2}, \left.\frac{\partial^2 z}{\partial y^2}\right|_{p=p3}, \left.\frac{\partial^2 z}{\partial xy}\right|_{p=p1}, \left.\frac{\partial^2 z}{\partial xy}\right|_{p=p2}, \left.\frac{\partial^2 z}{\partial xy}\right|_{p=p3};$$

- The partial derivative of the function differentiated in the normal direction to each side**,** $\mathbf{n \perp s}$**,** of the triangle. This is a polynomial of degree three, at most, in the variable measured in the direction of the side of the triangle (Akima 1978). These assumptions yield 3 additional conditions related to the three sides of the triangle**:**

$$\left.\frac{\partial z}{\partial n}\right|_{n\perp s1}, \left.\frac{\partial z}{\partial n}\right|_{n\perp s2} \text{ and } \left.\frac{\partial z}{\partial n}\right|_{n\perp s3}.$$

To calculate the partial derivatives in every data point $\mathbf{P_k}$ **(k=1,2,3,...n;** where **n** is the total number of data points) one has to use the point itself and its **nc** closest neighbors. Akima suggests a number among 3 and 5 for nc.

The evaluation of the partial derivative on a given data point $\mathbf{P_k}$ begins with the determination of the vector normal to the surface at this point. This vector is calculated by performing the summation of the vectors obtained from the vector product of every pair of vectors formed by $\mathbf{P_k}$

and two different neighbors points. The vector product of $\mathbf{P_k = (x_k, y_k, z_k)}$ and two of its neighborhood, $\mathbf{P_i = (x_i, y_i, z_i)}$ **and** $\mathbf{Pj = (x_j, y_j, z_j)}$ $\mathbf{\iota \neq \varphi}$, can be evaluated by the following equations:

$$\mathbf{dz_{ikj} = (x_i - x_k)(y_j - y_k) - (y_i - y_k)(x_j - x_k)} \quad \textbf{(8)}$$

$$\mathbf{dx_{ikj} = (y_i - y_k)(z_j - z_k) - (z_i - z_k)(y_j - y_k)} \quad \textbf{(9)}$$

$$\mathbf{dy_{ikj} = (z_i - z_k)(x_j - x_k) - (x_i - x_k)(z_j - z_k)} \quad \textbf{(10)}$$

where $\mathbf{dz_{ikj}}$, $\mathbf{dx_{ikj}}$ and $\mathbf{dy_{ikj}}$ are the three components of the vector product.

If $\mathbf{dz_{ikj} < 0}$ it is necessary to multiply the elements $\mathbf{dz_{ikj}}$, $\mathbf{dx_{ikj}}$ **and** $\mathbf{dy_{ikj}}$ by -1 to assure that the direction of the vector normal to the surface is positive. To calculate the gradient vector, in the **x** and **y** directions, it is necessary to solve the following equations:

$$\left.\frac{\partial z}{\partial x}\right|_{p=pk} = \sum_{i=0}^{nc-2}\sum_{j=i+1}^{nc-1} dx_{ikj} \Big/ \sum_{i=0}^{nc-2}\sum_{j=i+1}^{nc-1} dz_{ikj} \quad \textbf{(11)}$$

$$\left.\frac{\partial z}{\partial y}\right|_{p=pk} = \sum_{i=0}^{nc-2}\sum_{j=i+1}^{nc-1} dy_{ikj} \Big/ \sum_{i=0}^{nc-2}\sum_{j=i+1}^{nc-1} dz_{ikj} \quad \textbf{(12)}$$

where $\mathbf{dz_{ikj}}$, $\mathbf{dx_{ikj}}$ and $\mathbf{dy_{ikj}}$ are evaluated by equations 8, 9 and 10 respectively.

A similar approach can be used to calculate the second derivatives. In this case the coordinates $\mathbf{x_i}$, $\mathbf{y_i}$ **and** $\mathbf{z_i}$ **are** substituted by $\left.\frac{\partial z}{\partial x}\right|_{p=pi}$, $\left.\frac{\partial z}{\partial y}\right|_{p=pi}$ and **1** in equations 8, 9 and 10.

2.1.3. *Stochastic fitting*

The most popular stochastic models to represent curves and surfaces are based on fractal concepts. **A fractal** *is a geometrical or physical structure having an irregular or fragmented*

shape at all scales of measurement. In addition, a fractal is *self-similar* meaning that each part of its structure is similar to the whole.

Smoothed curves and surfaces are subjects of Euclidean geometry, and are adequate to represent artificial shapes like parts of mechanical and aeronautical projects, furniture, toys, etc.. Natural objects like clouds, coastlines and mountains have irregular or fragmented features. These are better represented by the Fractal geometry that was first formalized by Mandelbrot (1982).

Natural phenomena are not exactly self-similar, but *statistically self-similar*, i. e. each part of the structure is statistically (averages and standard deviations) similar to the whole. Indeed, real objects often look similar to pieces of themselves when examined at different cartographic scales and have forms that manifest significant randomness. Polidori (1991), Finlay (1993) and Fournier (1982) deal with the description of terrain as a fractal surface.

Fractal dimension (D) is an index that measures the *complexity* or *irregularity* of a graphic object (curve, surface, etc.) that represents a phenomenon. The fractal dimension of a line can be determined by the relation:

$$\mathbf{D = \log (n_i / n_j) / \log (s_j / s_i)} \qquad \mathbf{(13)}$$

where: $\mathbf{s_i}$ and $\mathbf{s_j}$ are two different step sizes used to measure the length of a line and;

$\mathbf{n_i}$ and $\mathbf{n_j}$ are the number of $\mathbf{s_i}$ and $\mathbf{s_j}$ steps to span the line respectively.

Lam (1993) presents some measurement methods to evaluate the fractal dimension for curves and surfaces.

Brownian motion is the most popular model used to perform fractal interpolations from a set of samples. Brownian motion, first observed by Robert Brown in 1827, is the motion of small

particles caused by continual bombardment by other neighboring particles. Brown found that the distribution of the particle position is always *Gaussian* with a variance dependent only on the length of the time of the movement observation **(**Finlay 1993).

The **Fractional Brownian motion (fBm),** derived from Brownian motion, can be used to simulate topographic surfaces. fBm provides a method of generating irregular, self-similar surfaces that resemble topography and that have a known fractional dimension (Goodchild 1987). The fBm functions can be characterized by variograms (graphic that plots the phenomenon variation against the spatial distance between two points) of the form:

$$\mathbf{E[(z_i - z_j)]^2 = K*(d_{ij})^{2H}} \qquad \mathbf{(14)}$$

where **E** denotes the statistical expectation**,** $\mathbf{z_i}$ and $\mathbf{z_j}$ represent the heights of the surface at the points **i** and **j** and $\mathbf{d_{ij}}$ is the spatial distance between these points**. K** is a constant of proportionality and is related to a vertical scale factor **S** that controls the roughness of the surface**. H** is a parameter in the range 0 to 1**. H** describes the *relative smoothness at different scales* and has the following relation with the fractal dimension **D:**

$$\mathbf{D = 3 - H} \qquad \mathbf{(15)}$$

When **H** is .5 we get the pure Brownian motion. The smaller **H**, the larger **D** and the more irregular is the surface. On the contrary, the larger **H,** the smaller **D** and the smoother the surface (Goodchild 1980).

Fournier (1982) presents recursive procedures to render curves and surfaces based on stochastic models. He describes two methods to construct two-dimensional fractal surface primitives. The first one is based on a *subdivision of polygons* to create fractal polygons while the second approach is based on the *definition of stochastic parametric surfaces.*

The *subdivision of polygons* is based on the *fractal polyline subdivision* method. A fractal polyline subdivision is a recursive procedure that interpolates intermediate points of a polyline. The algorithm recursively subdivides the closest extreme intervals and generates a scalar value at the midpoint which is proportional to the current standard deviation σ_c times the scale or roughness factor **S.** So, the z_m value of the middle point between two consecutive points**, i** and **j,** of a polyline is determined by the following equation:

$$z_m = (z_i + z_j)/2 + S*\sigma_c *N(0,1) \quad (16)$$

where σ_c varies according to equation 14 and **N(0,1)** is a Gaussian random variable with zero mean and unit variance**.** Press (1988) presents some algorithms to calculate random numbers with different distributions including the Gaussian.

The subdivision of polygons method is suitable to create stochastic surfaces based on TIN digital models. Each triangle of the TIN model can be subdivided into four smaller triangles by connecting the midpoints of the triangles. The z value of the midpoints is calculated by the fractal polyline subdivision method presented above. The subdivision can be continued until the area or a side of the current triangle reaches a predefined limit. So the original triangle is transformed into a fractal triangle whose irregular surface consists of many small triangular facets. Some care must be taken to ensure internal and external consistency among the adjacent triangles during the construction of the stochastic TIN model.

As pointed out by Fournier, the presented methods for rendering curves and surfaces are satisfactory approximations of fractional Brownian motion. They allow us to create realistic surfaces in faster time than with exact calculations. Another advantage of these approaches is the possibility of computing surfaces to arbitrary levels of detail without increasing the database.

Figure 2 illustrates the behavior of fractal curves created using fractional Brownian motion, different values of **H,** and a constant vertical scale factor. The curves were rendered using the fractal polyline subdivision method**.**

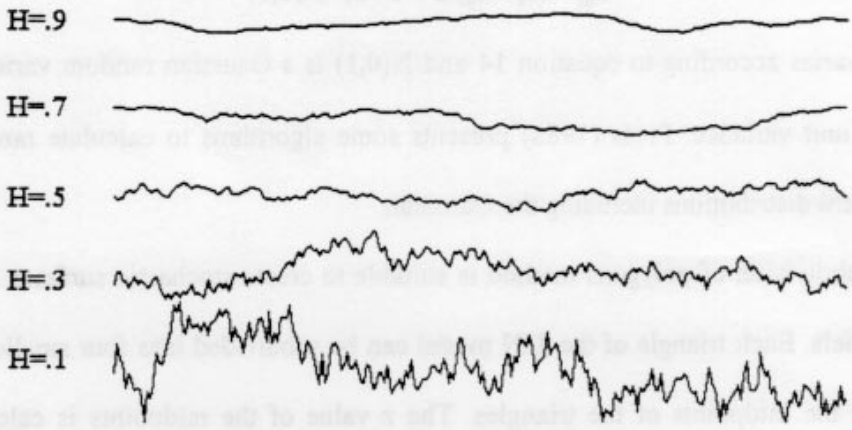

Figure 2. Stochastic curves rendered for different values of the parameter H.

3. Methodology

This section describes the methodology used to analyze and to compare the different approaches for surface fitting on TIN models.

We can divide the methodology into five steps:

1. Definition of the input sample set;
2. Construction of a TIN model;

3. Surface fitting for a mathematically defined function;
4. Surface fitting for a DEM-USGS data file and;
5. Statistical analysis for rectangular regular grid models.

3.1. *Definition of the input sample set*

The first step for modeling surfaces is the definition of the input sample set that will be used to construct the surface. This sample set must be representative of the phenomenon to be modeled.

To compare the two initial approaches for surface fitting, linear and quintic, we chose two different patterns. The first pattern of comparison was the following mathematically defined function that will be called the *sinc function* hereafter:

$$\mathbf{z(x, y) = sinc(d_i) = sin(d_i)/d_i} \qquad \mathbf{(17)}$$

The parameter $\mathbf{d_i}$ in equation 17 means the bi-dimensional euclidean distance from a generic point $\mathbf{P_i\ (x_i, y_i)}$ to the point origin $\mathbf{P_0(0., 0.)}$, that is, the $\mathbf{d_i}$ parameter is defined by the equation:

$$\mathbf{d_i^2 = x_i^2 + y_i^2} \qquad \mathbf{(18)}$$

This is an interesting test function because it has continuity of degree greater than 0, i. e. is a smooth function, and has intrinsic positive and negative derivatives.

A DEM-USGS data file was used as the second pattern to evaluate the results with real elevation data. In this case the stochastic approach was included in the analysis because of the characteristics of the data and the interpolator.

The sample set was defined by choosing the very important points (**VIP**) from rectangular regular grids obtained from the sinc function and from the DEM-USGS data file. To get the very

important sample points from a rectangular regular grid, a variation of the algorithm proposed by Chen (1987) was used. His method is based on a numerical evaluation of the importance of each element of the rectangular grid. The algorithm assumes that the greater the elevation difference between the sample point and its 8 neighbors, the more important it is.

The Chen algorithm was improved by giving a high value, greater than the maximum possible, to the local maximum or minimum grid points. This assumption guarantees that all peaks and pits, including the small ones, will be included among the very important points.

3.2. *TIN model construction*

The next step involves the use of the sample set to construct the basic structure of the DTM model. Here the input samples were transformed on the vertices of the triangles of a TIN model.

Some important characteristics of the TIN algorithm implemented are:

- It is an incremental algorithm, i. e. the sample points are introduced, one at a time, into the previous triangulation which is then refined;
- It creates a Delaunay triangulation;
- It uses the Delaunay empty circle criterion locally during the incremental process in order to avoid local thin triangles and;
- It uses a recursive function to create the final Delaunay triangulation.

Figure 3 depicts six Delaunay triangulations constructed from 93, 253, 505, 757, 997, and 2017 input samples. These input points were defined by the algorithm that chose the very important points from a rectangular regular grid. The z value for each point of the grid was obtained from the sinc function.

3.3. *Surface fitting for mathematical function data*

The linear and quintic interpolation approaches were implemented following the concepts presented in sections 2.1.1 and 2.1.2 respectively. The linear approach depends only on the vertices of the triangle and is straightforward. To implement the quintic approach two important details of implementation can be noted here:

- The derivatives at the vertices of the triangles were evaluated and stored during the quintic interpolation fitting. This avoided the unnecessary calculation of derivatives at the vertices of triangles that were not used during the process of rectangular grid creation.
- To evaluate the derivative in the vertices of a chosen triangle it was necessary to find the neighborhood of each vertex point that formed the triangle. This was accomplished using the vertices of the triangles that were neighbors of the chosen triangle**.**

The linear and quintic interpolation functions were compared using the sinc function. To perform this task rectangular grids (50 x 50 points) were constructed using z values calculated from the sinc function, from the linear interpolation and from the quintic interpolation. In addition, two more grids were created representing the difference between the linear and the original surface, and the quintic and the original surface.

Figures 4 and 5 show the perspective view of rectangular grids fitted by linear and Akima methodologies. They also show the difference between those models and the model defined by the sinc function.

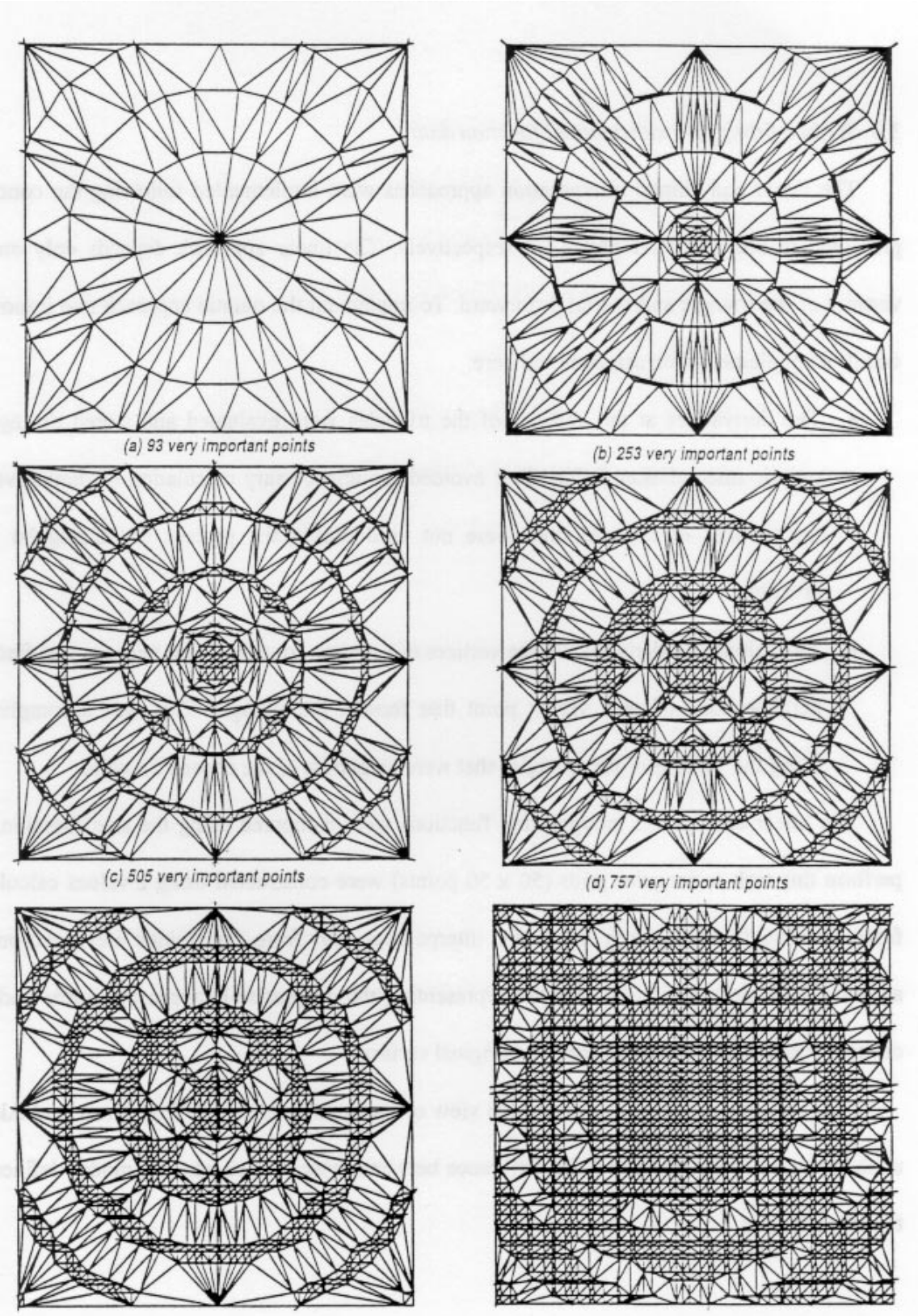

Figure 3. TINs constructed using very important points of the sinc function.

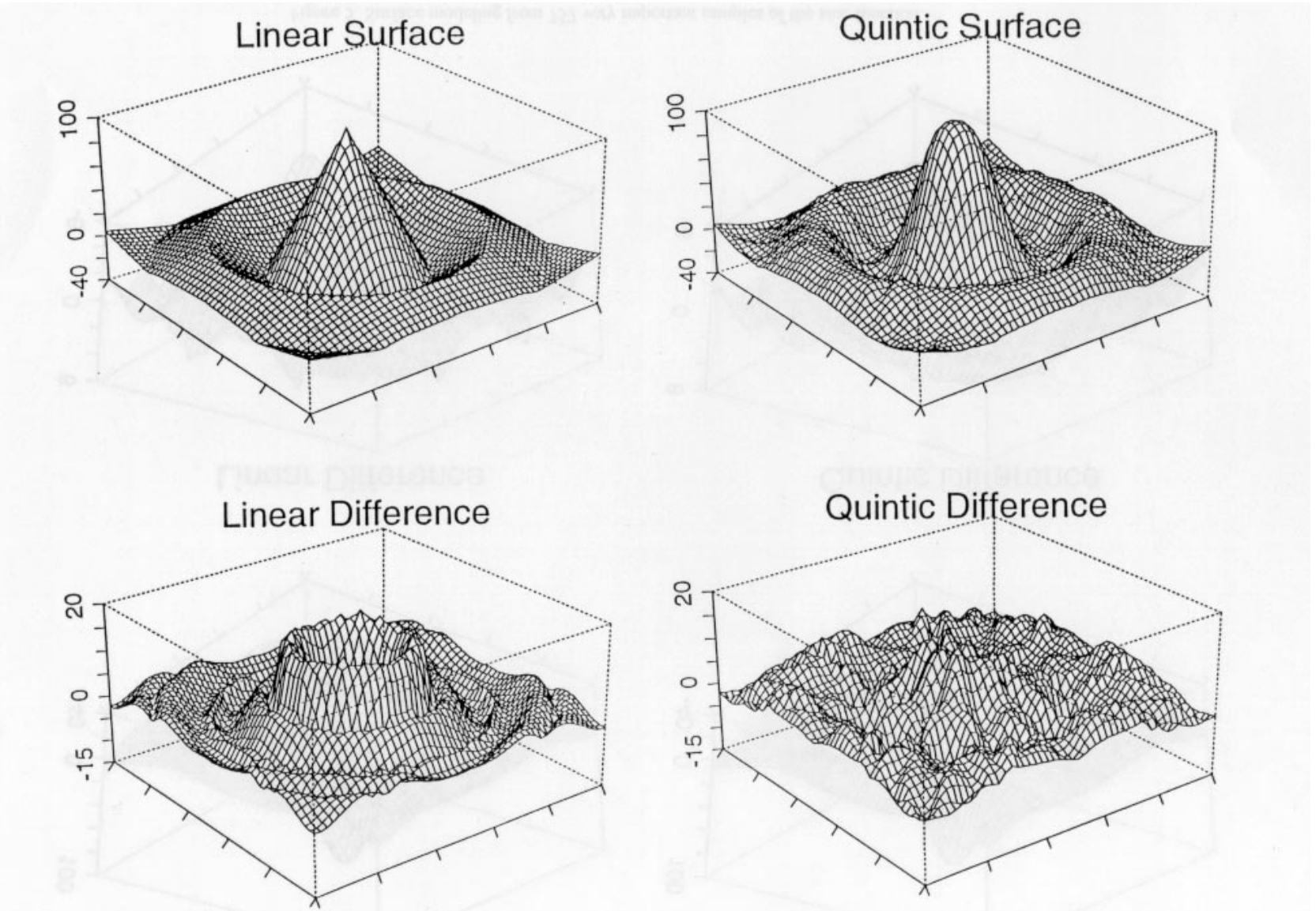

Figure 4. Surface modeling from 93 very important samples of the sinc function.

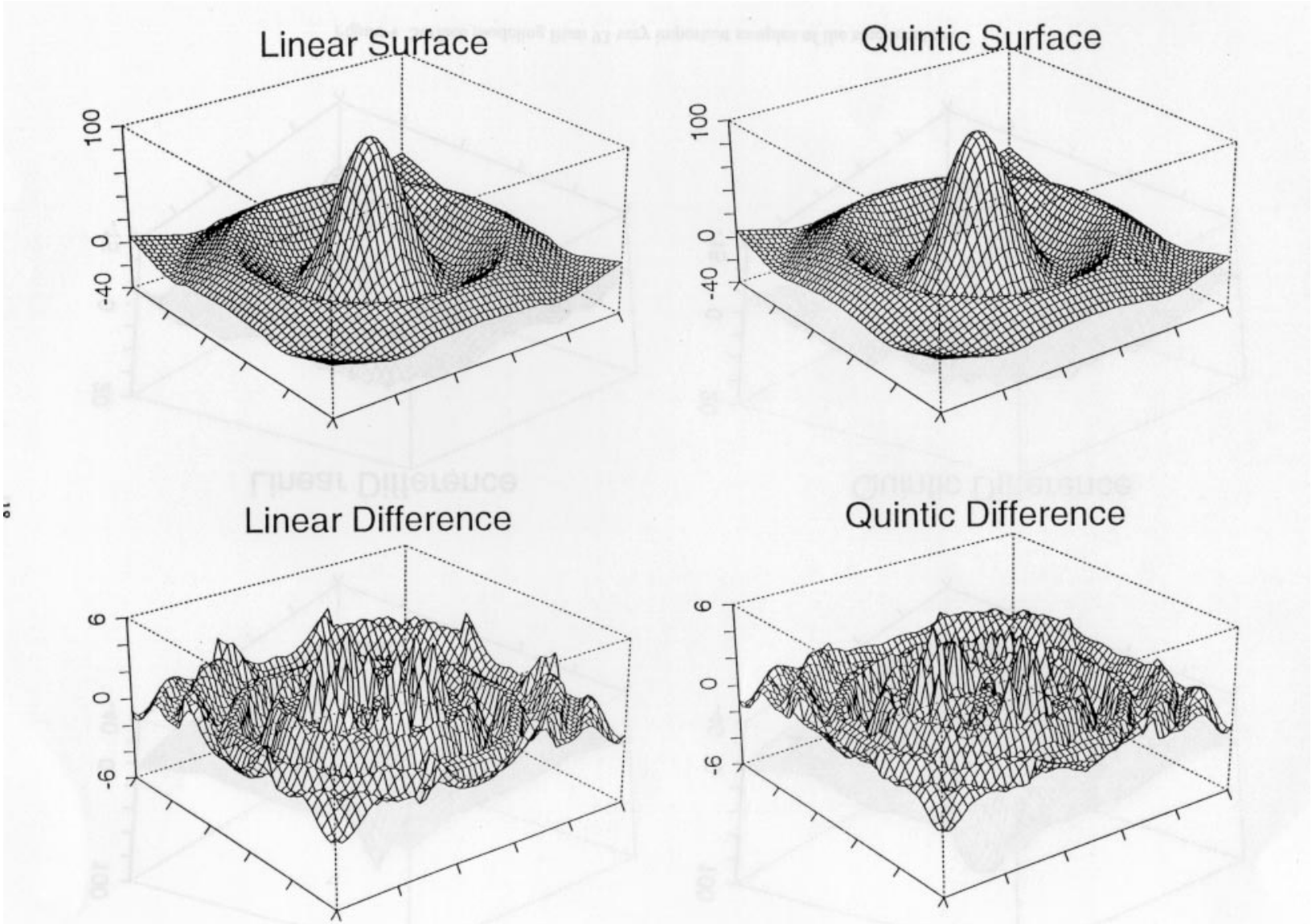

Figure 5. Surface modeling from 757 very important samples of the sinc function.

3.4. *Surface fitting for DEM-USGS data*

The sequence presented in section 3.3 was repeated using DEM-USGS data instead of the data from the sinc function. Figure 6 shows a Delaunay triangulation constructed with 2917 very important points from a DEM data file.

The DEM-USGS data used is from the Virginia, Minnesota (USA), region whose geographic coordinate reference is: N 43^{o}30' and W 92^{o}30'. The UTM zone, number 15, has the following bounding box planimetric coordinates (in meters): NW(528175, 5274471); NE(537568, 5274524); SW(528242, 5260579) and; SE(537658, 5260632). The objective was to compare the linear and quintic interpolators using real elevation data. In addition, a stochastic interpolator was included to create surfaces with more natural looks.

The stochastic method, used to estimate the z values of the rectangular grid, was based on the polygon subdivision approach presented in Fournier (1982). The method begins finding the current triangle $\mathbf{T_c}$, of the original TIN model, that contains the grid point $\mathbf{P_i}$ $\mathbf{(x_i, y_i, z_i)}$. Then the triangle $\mathbf{T_c}$ is subdivided recursively in four smaller triangles by connecting the midpoints of its sides. The z values of these midpoints are defined by a fractal polyline subdivision approach described in section 2.1.3. A new triangle $\mathbf{T_c}$, that contains the point $\mathbf{P_i}$, is chosen among the four smaller triangles. The subdivisions continue until the point $\mathbf{P_i}$ is within a defined proximity criterion of one of the vertices of the triangle $\mathbf{T_c}$. When the proximity is reached one can define $\mathbf{z_i}$ equal to the **z** of this vertex.

Figure 7 shows perspective projections of grid models constructed with samples from DEM-USGS data using linear, quintic and stochastic interpolators. Figure 8 presents stochastic models of the DEM-USGS data constructed with different values of parameter **H**.

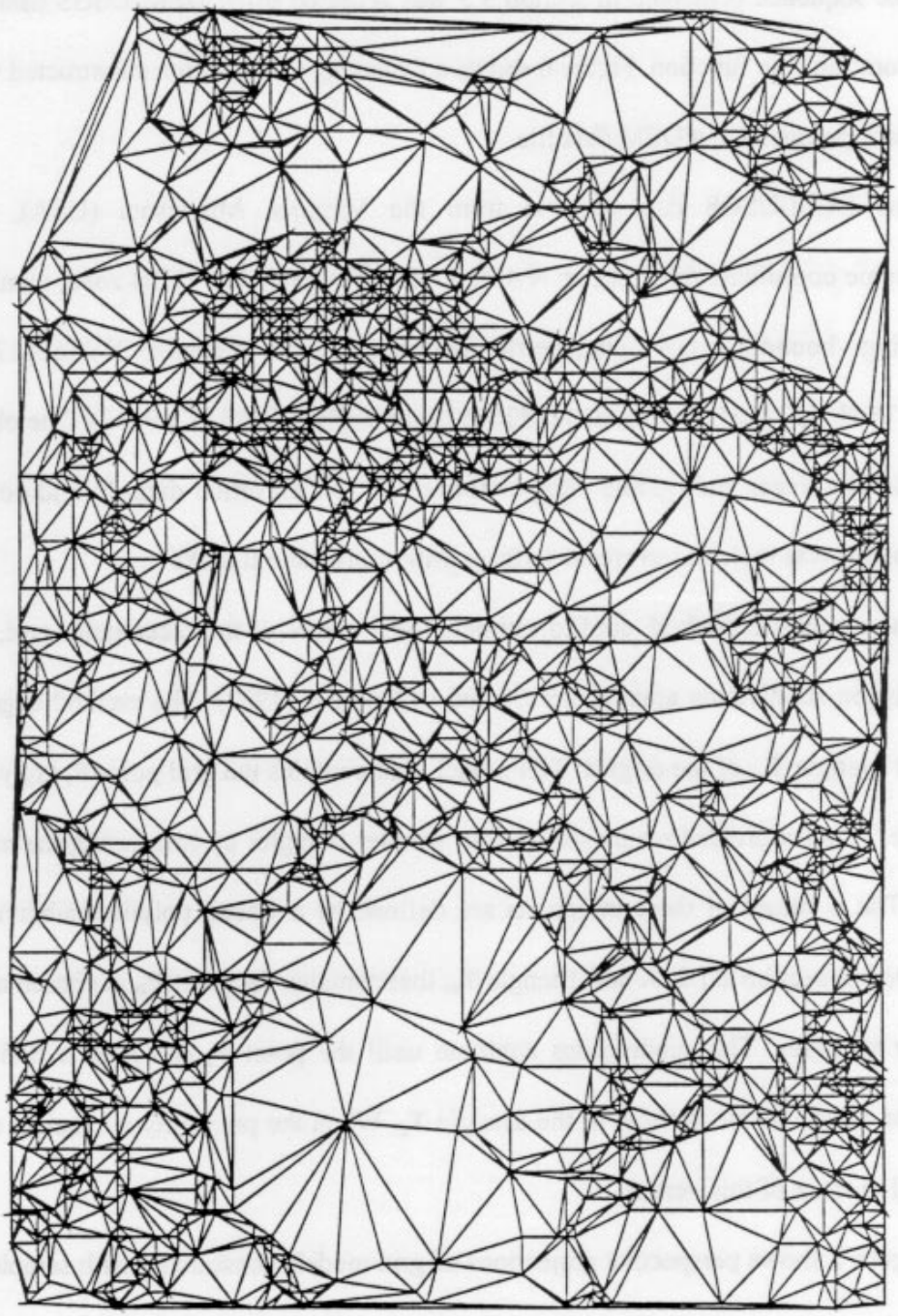

Figure 6. Triangulation constructed from 2917 very important points of the DEM data file.

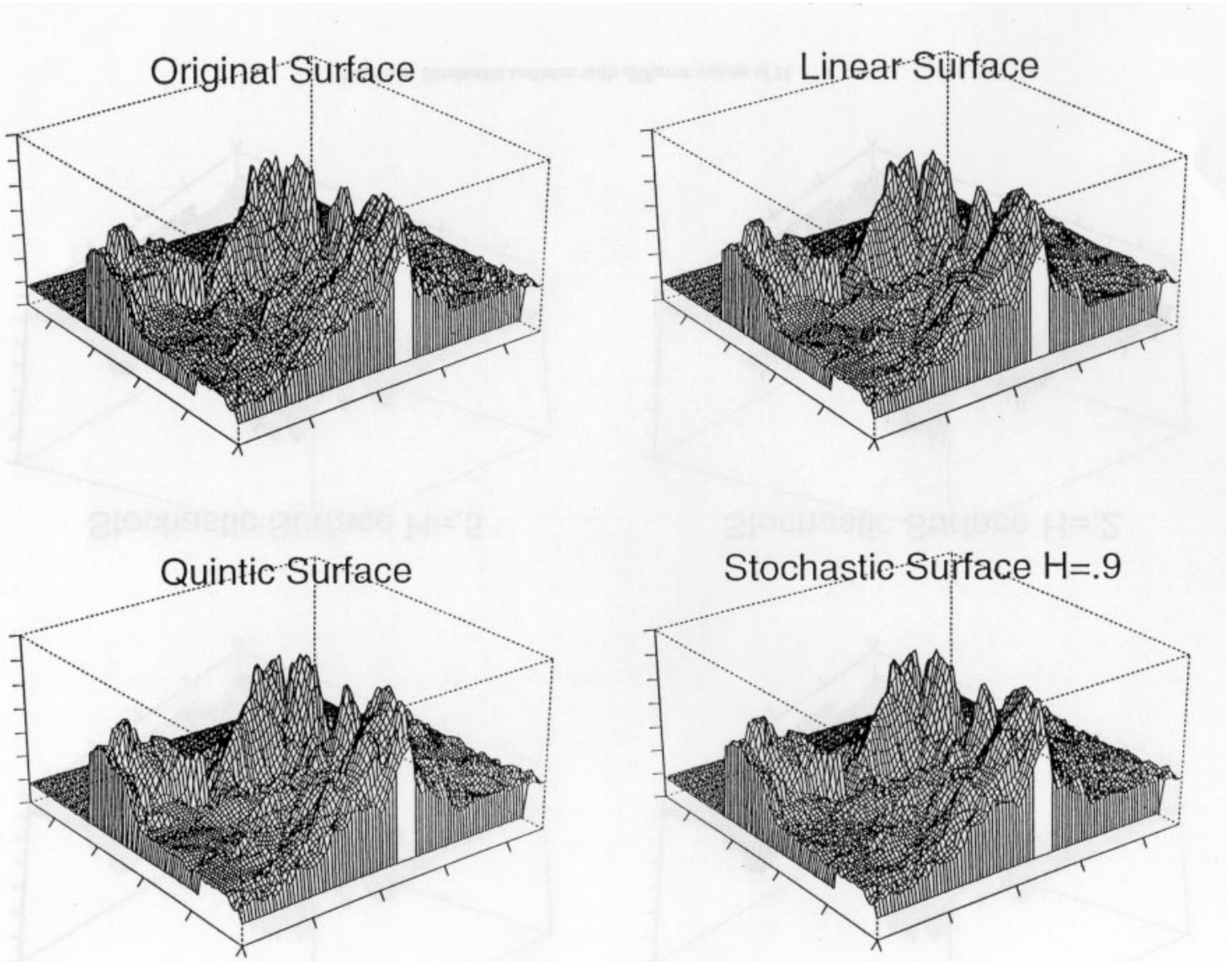

Figure 7. Surface modeling using 2917 very important points of the DEM data file.

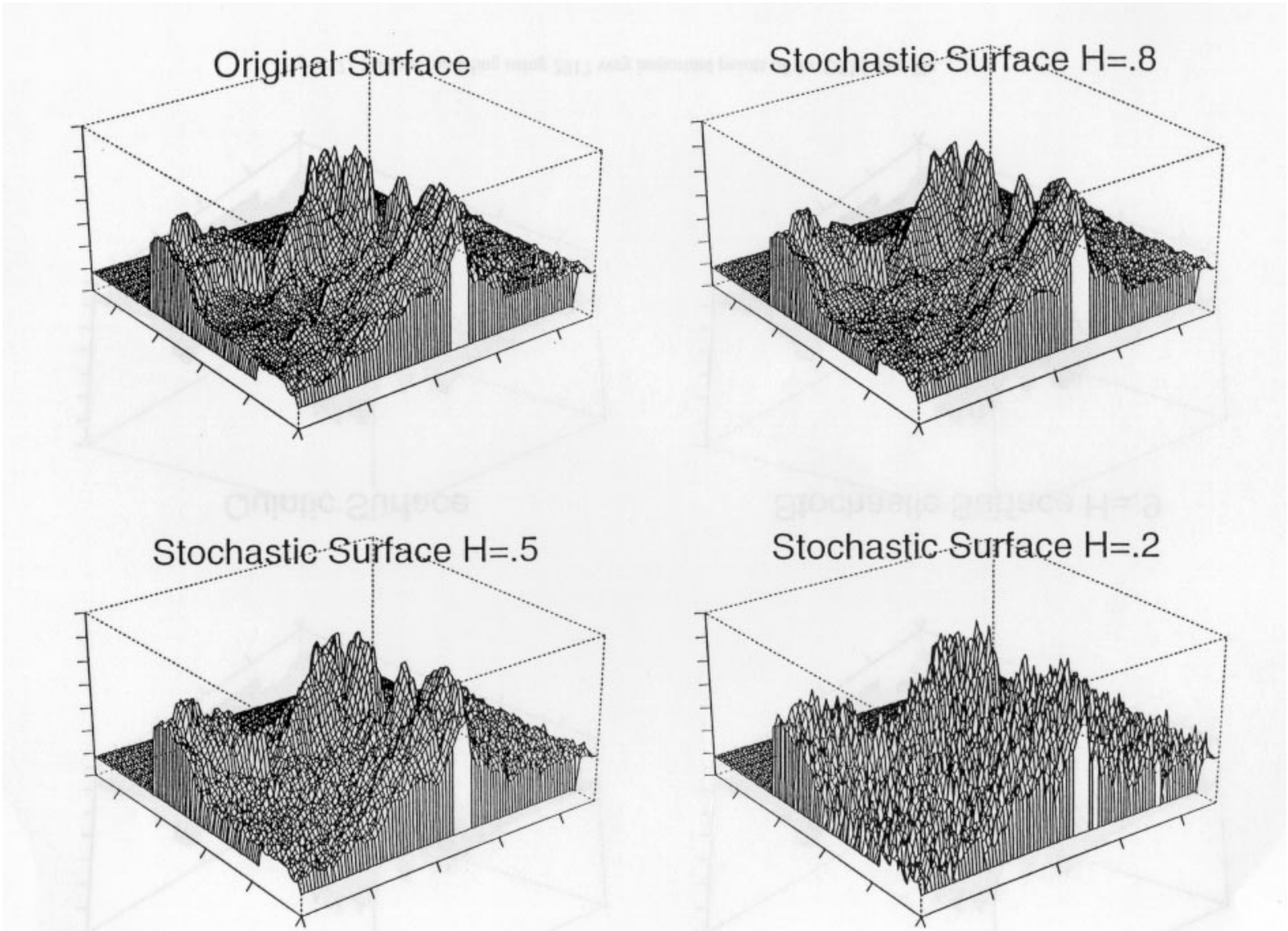

Figure 8. Stochastic surfaces with different values of H.

3.5. *Statistical analysis of the grid models*

In order to perform a quantitative analysis of the surfaces rendered by the three interpolator approaches, we compared them with the real, or original, surfaces. This was achieved by comparing the regular rectangular grids created by the interpolators with the real grids.

For each point of a regular rectangular grid we can calculate the *error function* **Er** defined as the difference between the *real elevation* $\mathbf{z_r}$ and the *estimated elevation* $\mathbf{z_e}$ in that point. The **Er** function is defined as:

$$\mathbf{Er} = \mathbf{z_r} - \mathbf{z_e} \tag{19}$$

Suppose that we have **npt** points representing the surface. To evaluate the *average* (**Av**), *variance* (**Var**) and *standard deviation* (**Std**) of the error function (**Er**) we can use the following equations:

$$\mathbf{Av} = \left(\sum_{k=0}^{npt-1} \mathbf{Er_k} \right) \Big/ \mathbf{npt} \tag{20}$$

$$\mathbf{Var} = \left[\left(\sum_{k=0}^{npt-1} \mathbf{Er_k^2} \right) - \mathbf{npt} * \mathbf{Av}^2 \right] \Big/ \left(\mathbf{npt} - 1 \right) \tag{21}$$

$$\mathbf{Std} = \sqrt{\mathbf{Var}} \tag{22}$$

We used the sinc function and the DEM-USGS data file as source of real data $\mathbf{z_r}$ on each point of the grid. The value of $\mathbf{z_e}$**,** in each point of the grid, was estimated using the linear, quintic and stochastic interpolators.

4. Results and analysis

Table 1 contains the results of the statistical analysis, in meters, of the error function defined by the linear and quintic interpolators. The sample set was obtained from the sinc function. The range in elevation is about 120 m.

Table 2 presents the statistical results, in feet, obtained when using very important samples from DEM-USGS data files. In the studied area the elevation varies 105 feet approximately.

A *quantitative* analysis of the figures and the tables presented on sections 3 and 4, respectivelly, leads to the following notes:

- An already predicted result is that the linear interpolator is computationally more efficient than the quintic interpolator. This is easy to explain because of the number of calculations required for each approach. For the quintic approach, the necessity to calculate the first and second derivatives in the samples creates a significant time overhead.
- Table 1 shows that an increase in the number of input samples leads to more accurate models. However, satisfactory results, depending on the requirements, can be obtained after reducing the sample set by a VIP algorithm. This reduction saves memory space and can increase substantially the speed of the programs designed to create the digital models. The triangulation shown on Figure 6 was constructed with approximately 2% of the total number of samples contained in the original DEM-USGS data file.

From Table 1 we can conclude that the quintic interpolator performs better than the linear interpolator for samples chosen from the sinc function. This was expected because the sinc surface has continuity greater than 0.

Interpolator	Number of Samples	Average	Variance	Std Deviation
linear	93	0.72	19.60	4.43
quintic	93	0.36	10.94	3.31
linear	253	0.42	12.22	3.50
quintic	253	0.49	6.93	2.63
linear	505	-0.39	3.97	1.99
quintic	505	-0.23	2.49	1.58
linear	757	-0.22	1.81	1.35
quintic	757	-0.21	0.96	0.98
linear	997	-0.35	1.09	1.04
quintic	997	-0.37	0.62	0.79
linear	2017	0.03	0.06	0.24
quintic	2017	0.00	0.01	0.11

Table 1. Statistical analysis of the error function for very important samples from the sinc function

Interpolator	Average	Variance	Std Deviation
Linear	.79	7.97	2.82
Quintic	.78	9.27	3.04
Stochastic H=.9	.78	8.21	2.86
Stochastic H=.5	.82	9.54	3.09
Stochastic H=.2	.9	23.27	4.87

Table 2. Statistical analysis of the error function for very important samples from the DEM data

- As shown in Table 2, no significant statistical difference was found between the linear and quintic approaches to model DEM-USGS data. The important question here is: Does the real elevation surface have smooth behavior? If the elevation data has continuity of order 0, that means continuous but not differentiable, it is satisfactory to use a linear interpolator instead of high degree polynomial interpolators
- Table 2 also shows that the error analysis of the stochastic approach, when H=.9, gets similar results to the linear and the quintic methods. So, the stochastic methods can be successfully used when the real surface represents a natural phenomenon like elevation. The major problem seems to be the definition of the appropriate parameters H and S to best represent the variations of the real surface.

A *qualitative* analysis of the figures presented on section 3 leads to the following considerations:

- From Figures 4 and 5 we see that the greater the number of very important points the better is the appearance of the final modeled surface. In addition, these figures show the differences between the fitted models and the model defined by the sinc function. The latter gives us an idea of the spatial distribution of the error function along the surface.
- Figures 4 and 5 also show us that, for the same sample set of the sinc function, the model fitted by a quintic interpolator is smoother than the model fitted by a linear interpolator.
- Figure 7 reveals that we get a more natural looking surface by using stochastic interpolator, compared with linear and quintic interpolators, although the statistical analysis does not confirm this improvement. In addition, the fractal behavior is more

apparent just on the areas with little density of samples. In these regions it is common for artifacts, like flat or too smoothed surfaces, to appear when linear and quintic interpolators are used.

- As expected, the Figure 8 shows that different values of parameter H, and therefore different fractal dimensions, lead to different surface representations. The smaller the H, the more irregular is the surface, and vice-versa.

5. Concluding remarks

To compare the surfaces fitted by linear, quintic and stochastic methods we studied and implemented an algorithm to chose the very important points from a rectangular grid model, an algorithm to create the Delaunay triangulation, and three interpolators that fit linear, quintic and stochastic surfaces for TIN models. The algorithms were implemented in the C programming language in a UNIX operational system environment. In addition, perspective projections and statistical tables were created to accomplish the qualitative and quantitative analysis of the models rendered.

The most important conclusion the presented results is that the quality of a digital terrain model depends on the type of object, or surface, that is been modeled. A representation that is useful for engineering object modeling may not be suitable to represent natural forms manipulated by geographers, for example. Specifically, linear interpolation is recommended for modeling natural terrain surfaces in GIS where the landscape is dominated by sharp ridges and incised valleys, and when interest lies in creating an accurate representation. Quintic interpolation is recommended for accurate modeling of natural terrain surfaces dominated by smoothing processes, such as glaciation, and also for modeling surfaces of other variables, particularly such

environmental variables as atmospheric temperature or groundwater depth, where physical laws tend to require higher order continuity. Finally, fractal interpolation is recommended for modeling natural terrain surfaces when interest lies in visualization, and when the parameters of the fractal interpolation can be adjusted to create a realistic-looking representation. Since all three methods achieved similar levels of accuracy against the admittedly limited testing carried out in this paper, it seems that the choice of interpolation method is more likely to be driven by conceptual understanding of the behavior of the real-world phenomenon, the need for credible visualization, and the practical limitations of software and computing resources, than by strict concern for accuracy.

Future research topics, to improve this work, should address the following questions: What are the errors involved in considering the DEM-USGS data as good representations of real elevation surfaces? and, How can we calculate the fractal dimension from a sample set to get a more natural look for the modeled surface?

References

AKIMA H., 1975, A method of bivariate interpolation and smooth surface fitting for values given at irregularly distributed points. Office of Telecommunications Report 75-70, U.S. Govt. Printing Office, Washington DC.

AKIMA H., 1978, A method of bivariate interpolation and smooth surface fitting for irregularly distributed data points. *ACM Transactions on Mathematical Software*, 4, 148-159.

BURROUGH, P. A., 1986, *Principles of Geographical Information Systems for Land Resources Assessment* (Oxford: Clarendon Press).

CHEN Z. and GUEVARA J. A., 1987, Systematic selection of very important points (VIP) from digital terrain model for constructing triangular irregular networks. In *Proceedings of Eight International Symposium on Computer-Assisted Cartography - AutoCarto 8,* (Baltimore: Mariland), pp. 50-56.

DE FLORIANI L. and PUPPO E., 1992, An on-line algorithm for constrained Delaunay triangulation. *CVGIP: Graphical Models and Image Processing*, 54, 290-300.

FALCIDIENO B. and SPAGNUOLO M., 1991, A new method for the characterization of topographic surfaces. *International Journal of Geographical Information Systems*, 5, 397-412.

FINLAY M. and BLANTON K. A., 1993, *Real-World Fractals* (New York: M&T Books).

FOURNIER A. , FUSSELL D. and CARPENTER L., 1982, Computer rendering of stochastic models. *Communications of the ACM*, 25, 371-384.

GOODCHILD M. F., 1980. Fractals and the accuracy of geographical measures. *Mathematical Geology*, 12, 85-98.

GOODCHILD M. F. and MARK D. M., 1987, The fractal nature of the geographic phenomena. *Annals of the Association of American Geographers*, 77, pp. 265-278.

LAM N. S. and DE COLA L., 1993, *Fractals in Geography* (Englewood Cliffs: Prentice Hall).

LANCASTER P. and SALKAUSKAS K., 1986, *Curve and Surface Fitting: An Introduction*. (London: Academic Press).

LEE J., 1991, Comparison of existing methods for building triangular irregular network models of terrain from grid digital elevation models. *International Journal of Geographical Information Systems*, 5, 267-285.

MANDELBROT B. B., 1982, *The Fractal Geometry of Nature* (New York: W. H. Freeman and company).

MCCULLAGH M. J., 1988, Terrain and surface modeling systems: theory and practice. *Photogrammetric Record*, 12, 747-779.

POLIDORI L., CHOROWICZ J. and GUILLANDE R., 1991, Description of terrain as a fractal surface and application to digital elevation model quality assesment. *Photogrametric Engeneering & Remote Sensing*, 57, 1329-1332.

PREPARATA F. P. and SHAMOS M. I., 1988, *Computational Geometry: An Introduction* (New York: Springer-Verlag).

PRESS W. H., FLAWNERY B. P., TEUKOLSKY S. A. and VETTERLING W. T., 1988, *Numerical Recipes in C The Art of Scientific Computing* (Cambridge: Cambridge University Press).

TSAI V. J. D. 1993, Delaunay triangulations in TIN creations: an overview and a linear-time algorithm. *International Journal of Geographical Information Systems*, 7, 501-524.

AN INCREMENTAL CONSTRAINED DELAUNAY TRIANGULATION

CARLOS A. FELGUEIRAS
MICHAEL F. GOODCHILD

Abstract: This work addresses the problem of constructing Triangular Irregular Network (TIN) models from irregularly distributed samples with constrained lines. The implementation of an incremental constrained Delaunay triangulation is described and compared qualitatively with the unconstrained Delaunay triangulation.

1. Introduction

The Triangular Irregular Network (TIN) models are very popular among the Geographical Information Systems (GISs) that are currently available in the market. Relevant information, such as slope, aspect, contour and visibility maps, can be extracted from this models for further integration with other information stored in the GIS database. The TIN models are used to represent the behavior of a phenomenon defined in a limited region of the earth surface. Elevation, temperature, population density, geological characteristic and others are among the most common phenomena represented by a TIN model. The spatial position of the phenomenon is represented in the xy coordinate system while the value of the phenomenon itself is represented in the z coordinate axis. Unless previously mentioned, this work will consider that the z coordinate is representing elevation.

Various commercial software packages provide the facility to construct Delaunay triangulations from a defined input sample set. When the sample set contains just sample points that do not have connections among them then the Delaunay TIN seems to be perfect to represent the surface behavior. Problems arise when the Delaunay TIN is created over a sample set that also contains opened lines and closed lines (polygons). Sometimes these lines are defined as barriers, ridge and river lines for example, that cannot be crossed by triangle edges. In another situation, as in contour lines, the triangles whose 3 vertices are in the same contour line, defining flat areas, must be avoided.

This work describes a method to construct an incremental Delaunay triangulation taking into account the constrained lines included in the sample set. The final triangulation is not strictly a Delaunay triangulation because it contains Delaunay triangles only in the areas far from constrained lines. Some authors call this network a *Constrained Delaunay Triangulation* (CDT) (Falcidieno 1990 and Floriani 1992).

The idea consists in constructing an initial Delaunay triangulation with the restriction that constrained segments, that are part of constrained lines, can not be crossed by any triangle edge. In a second step the initial triangulation is changed to avoid flat areas created by triangles whose three vertex points belong to the same contour line.

Section 2 presents some relevant concepts related to TIN models creation, including Delaunay triangulation and constrained Delaunay triangulation. Section 3 addresses some problems that occur when the TIN model is constructed using only the Delaunay conditions without considering constrained segments. Section 4 describes details of the implementation of a constrained Delaunay triangulation. Some qualitative results are shown and discussed in section 5.

Section 6 presents relevant conclusions and some suggestions for further research related to the subject of this work.

2. Triangular Irregular Network Models

A TIN represents a surface as a set of non-overlapping contiguous triangular facets, of irregular size and shape (Chen 1987). A TIN uses the data on the irregularly spaced samples as the basis of a system of triangulation (Burrough 1986). It is created directly from the set of samples, i. e. the vertices of the triangles are the samples. Commonly a TIN is constructed using the bidimensional projection of the sample points in the xy plane. Another popular digital terrain model is the regular rectangular grid that represents the surface as a regularly distributed set of points.

The main advantage of using TIN models, instead of rectangular grid models, is that the TIN can include a great number of points where the surface is rugged and changing rapidly and can contain a minimum of points in areas where the surface is relatively uniform (Kumler 1992). In addition, the points used to create the triangular network are the same input sample points while the network of a rectangular grid is formed by interpolated points, unless the sample points are located exactly in the vertices of the rectangular grid. Another reason for the interest in triangulation models has been that they are ideally suited to constrained information, like cliffs and break lines, insertion. If the locations of these special lines are entered as a logically connected set of data points, the triangulation process will include them and will automatically relate them to the rest of the data set (McCullagh 1988).

One of the disadvantage of TINs is the necessity to store the spatial position, xy, with each point of the network. This can be memory consuming if the number of points in the sample set is big. On the other hand, the spatial position of each point of a regular rectangular grid can be calculated since the geographic reference and the resolutions x and y of the grid were previously stored.

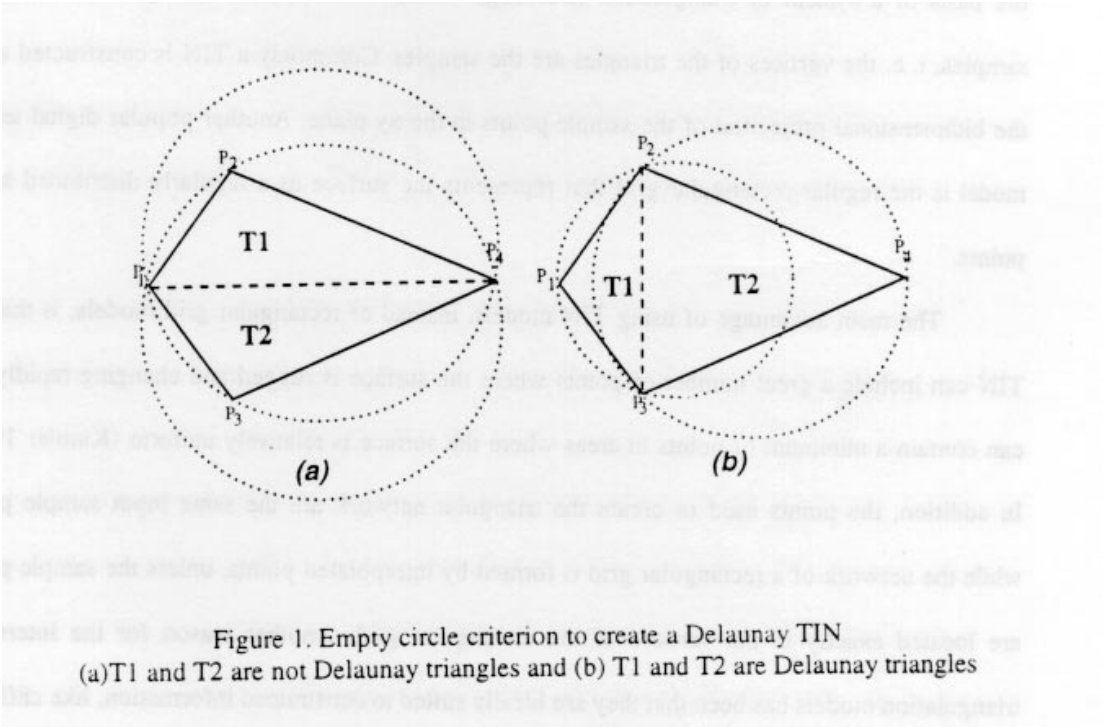

Figure 1. Empty circle criterion to create a Delaunay TIN
(a)T1 and T2 are not Delaunay triangles and (b) T1 and T2 are Delaunay triangles

The most popular TIN model, used in commercial software, is the *Delaunay triangulation*. The Delaunay TIN is the straight-line dual of the Voronoi diagram and is constructed by connecting the points whose associated Voronoi polygons share a common edge. The Delaunay TIN has the following properties:

- It is unique and;
- It maximizes the minimum internal angles of each triangle, i. e. the minimum angle of its triangles is maximum over all triangulations (Preparata 1988). This characteristic avoids the creation of thin triangles, i. e. each triangle is as equilateral as possible.

The circumference that passes through the three vertices of a Delaunay triangle does not contain any other sample point. This property is known as the *empty circle criterion* (Tsai 1993), or *Delaunay test*, and is used to construct the TIN model directly from the sample set. Figure 1 illustrates the use of the empty circle criterion condition to determine whether a triangle is Delaunay or not.

A *constrained triangulation* is a TIN constructed taken into account the topographic features, or the characteristic lines, of the surface. A good representation of the terrain should contain all the specific features of the surface shape including points (peaks and pits); lines (rivers, ridges and cliffs) and; surfaces (slopes, lakes). The segments that form the lines and the surfaces must me considered as barriers that can not be crossed during the process of triangulation. Some authors prefer to use the concept of visibility among the samples to construct the TIN. This means that a sample cannot be connected to other, to build an edge of a triangle, if there is a constrained segment between them.

A *constrained Delaunay triangulation* is a triangulation network that contains constrained edges and Delaunay edges. Constrained edges are forced to maintain the original characteristics of the terrain. The main objective of this work is to describe the implementation of a constrained Delaunay triangulation.

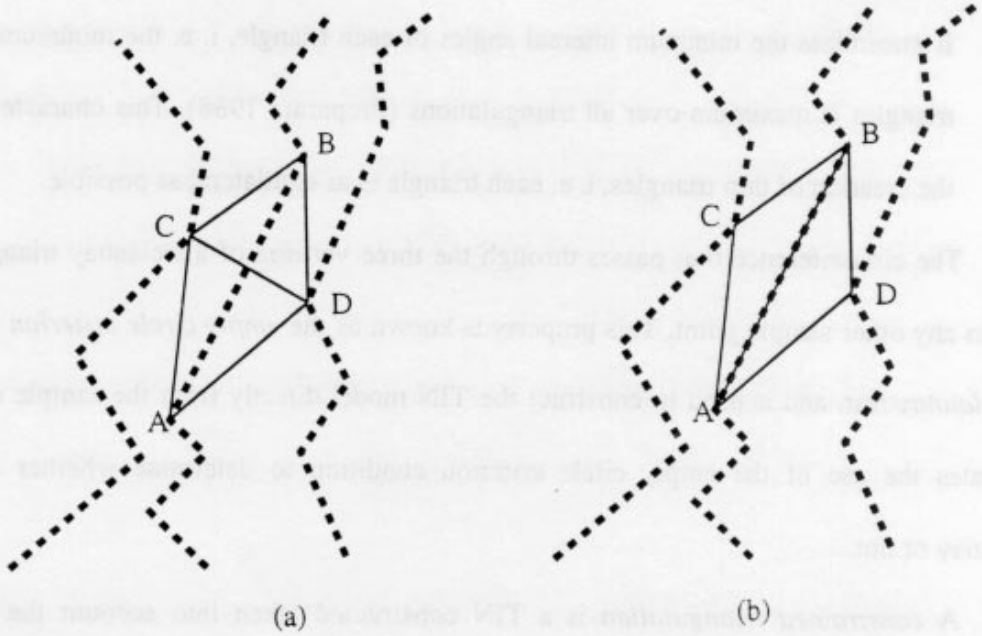

Figure 2. Triangles from characteristic lines (a) Delaunay triangulation and (b) constrained Delaunay triangulation

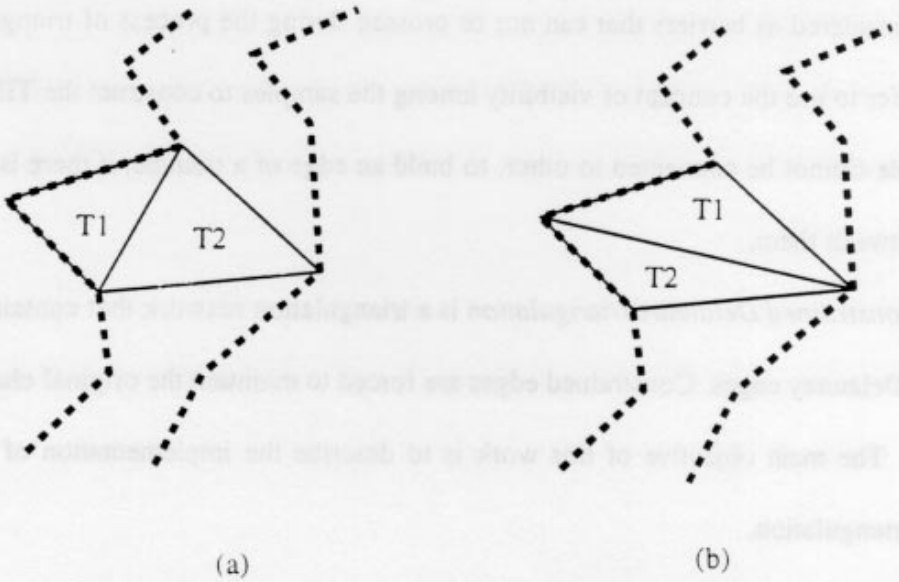

Figure 3. Triangles from contour lines (a) Delaunay triangulation and (b) constrained Delaunay triangulation

3. Problems created by non constrained Delaunay triangulation

This section describes some undesirable problems that occur when one creates a pure Delaunay triangulation, i. e. a Delaunay TIN without considering the topographic features of the surface.

3.1. *Crossing constrained segments*

Constrained segments are defined as segments created by consecutive points of the same constrained line. The figure 2(a) shows an example of Delaunay triangulation that creates undesirable artifacts in the surface to be represented. Suppose that the points A and B belong to a river line and the points C and D do not belong to the same river line and in addition they have elevations higher than those of the points A and B. The Delaunay triangulation, without constraints, creates a shape that is not acceptable in this surface because the river cannot climb a hill to follow its normal course. In this case it is better to create the triangles showed in the figure 2(b) even they fail to satisfy the empty circle criterion.

3.2. *Triangles created with all vertices from the same constrained line*

This problem is more harmful when the constrained lines are contour lines. The same z value is assigned to all the sample points that define a contour line. The figure 3(a) shows two triangles T1 and T2 of a Delaunay triangulation created without considering the contour lines as constrained lines. The triangle T1 is formed by three points of the same contour line. If one considers that each triangle defines a plane in the space, then the surface inside T1 is a flat surface (parallel to the xy plane). An alternative triangulation is shown in the figure 3(b). In these figures the triangles T1 and T2 are not Delaunay triangles but the flat triangular surface is avoided.

4. The incremental constrained Delaunay TIN algorithm

This section describes details of the data structure and the algorithm used to implement the incremental constrained Delaunay triangulation.

The constrained Delaunay triangulation was built using a two step algorithm. In the first step an incremental algorithm constructs an *initial constrained Delaunay triangulation*. The only restriction applied in this initial Delaunay triangulation is that the segments of the constrained lines cannot be crossed by triangular edges. In this step the points of the constrained lines are inserted first followed by the other samples. The second step is responsible for creating the *final constrained Delaunay triangulation* by eliminating flat triangles from the initial triangulation.

This implementation was performed in language C. The structure used to create a computer representation of the samples is shown below.

```
struct{
    int npt;
    float c[3];
    int line;
    int linetype;
    float dz1[2];
    float dz2[3];
} SAMPLE;
```

In the structure SAMPLE, the variable *npt* is the number of the point; the vector *c[3]* contains its coordinates x, y and z; *line* refers to the number of the line that contains the point (*line* = -1 means that the sample does not belong to any line); *linetype*, such as contour, ridge, river, fault, etc., is useful to define whether a sample line must be considered as constrained line or not; *dz1[2]* stores the first partial derivatives ($\delta z/\delta x$ and $\delta z/\delta y$) and; *dz2[3]* the second partial derivatives ($\delta^2 z/\delta x^2$, $\delta^2 z/\delta y^2$ and $\delta^2 z/\delta x \delta y$). The partial derivative information was not used in this implementation but will be helpful to fit smooth surfaces to the triangulation (Akima 1978 and

Lancaster 1986). The sample structure defined above is enough to allow one to discover if two points belong to the same constrained line and whether they are consecutive or not. These are the two basic conditions used to create the constrained TIN model presented in this work.

The structure that represents each triangle of the triangulation is presented below.

```
struct{
    int  v[3];
    int n[3];
    float  bb[4];
} TRIANGLE;
```

Each triangle is represented by: a point vector *v[3]* that stores the numbers of the points of its vertices; a neighbor vector *n[3]* that contains the numbers of its 3 neighbor triangles (-1 means no neighbor) and; a bounding box vector *bb[4]* that stores its spatial bounding box, x minimum, y minimum, x maximum and y maximum. The neighbor vector is useful to perform local triangle tests (as the empty circle criterion to create a Delaunay TIN) and to use recursive processes to propagate these tests to other neighborhoods. During the incremental process the bounding box of each triangle is used to accelerate the search for the triangle that contains one new sample.

Some important characteristics of the TIN algorithm implemented are:

- It is an incremental algorithm, i. e. the sample points are introduced, one at a time, into the previous triangulation which is then refined;
- The sample points of the constrained lines are inserted before the other samples;
- It creates a constrained Delaunay triangulation;
- It uses a constrained Delaunay empty circle criterion, or constrained Delaunay test, locally during the incremental process in order to avoid local thin triangles and;
- It uses a recursive function to create the final constrained Delaunay triangulation.

The general sequence of the incremental algorithm used to create the initial constrained Delaunay triangulation is presented below:

CONSTRAINED TIN FUNCTION
Begin
Calculate the bounding box rectangle of the samples

Create two initial triangles using the bounding box and one of its diagonals

For each new sample point Pn
Begin
Find the triangle Tp that contains Pn

Create three new triangles using Pn and the vertices of Tp

Apply the *constrained Delaunay test* between each new triangle and the respective neighbor of Tp

Discard the triangle Tp
End

Apply the constrained Delaunay test recursively in the current triangulation
End

The constrained Delaunay test, mentioned in the algorithm above, means that *the Delaunay test between two neighbor triangles will be applied only if their common edge **is not** formed by two consecutive points of the same constrained line.*

The next step of the algorithm is to change the initial triangulation to eliminate flat triangles. This is performed recursively between triangles that are neighbors. The test applied here is:

A common edge of two neighbor triangles must be changed if:

(a) the common edge is formed by two non consecutive points of a same constrained line and;

(b) the new edge is not formed by two non consecutive points of a same constrained line.

Once the result of the test above is true the common edge must be changed *even if the new triangles are not Delaunay*. As already mentioned in the section 3 this test is useful when the

sample set contains contour lines. This second step can be defined as optional by the user. For example, when the sample set does not include contour lines, the user would prefer to create the constrained triangulation without this last restriction.

5. Results

The pure Delaunay triangulation and the constrained Delaunay triangulation, presented in section 4, were applied to 3 different sample sets and the results are illustrated, compared and discussed in this section.

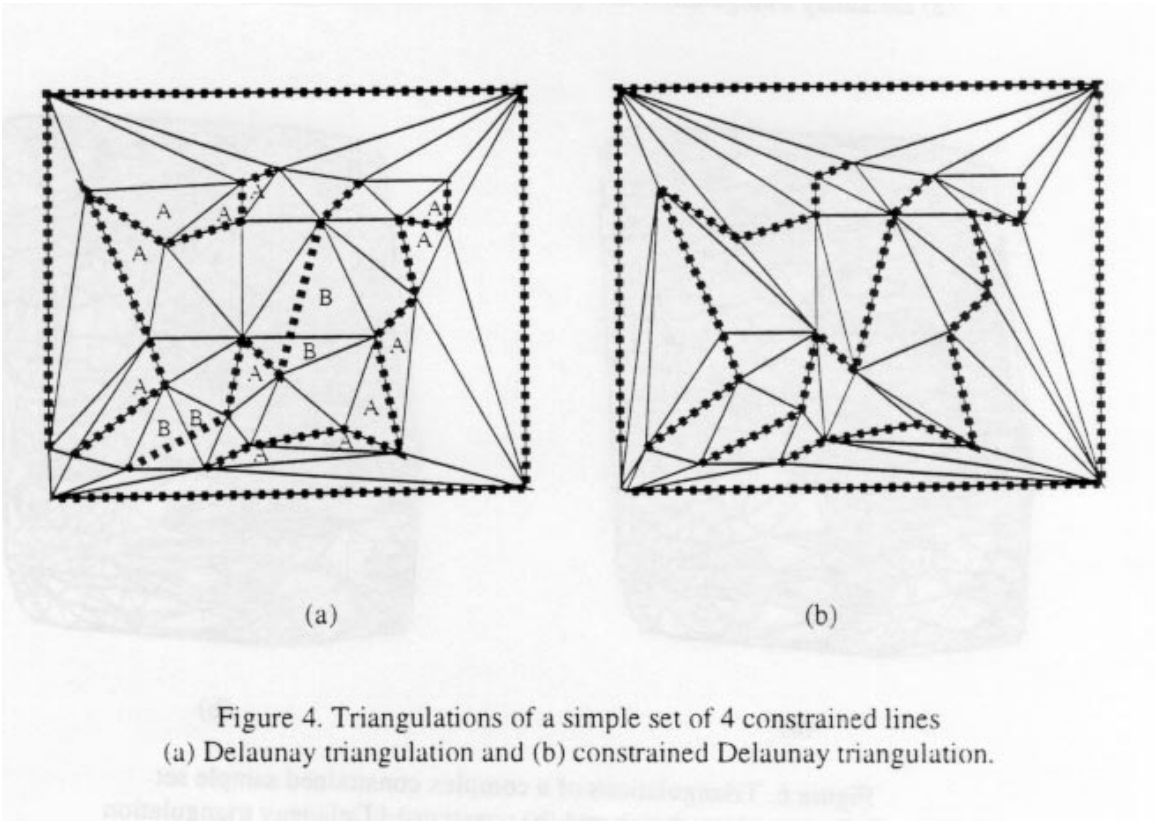

Figure 4. Triangulations of a simple set of 4 constrained lines
(a) Delaunay triangulation and (b) constrained Delaunay triangulation.

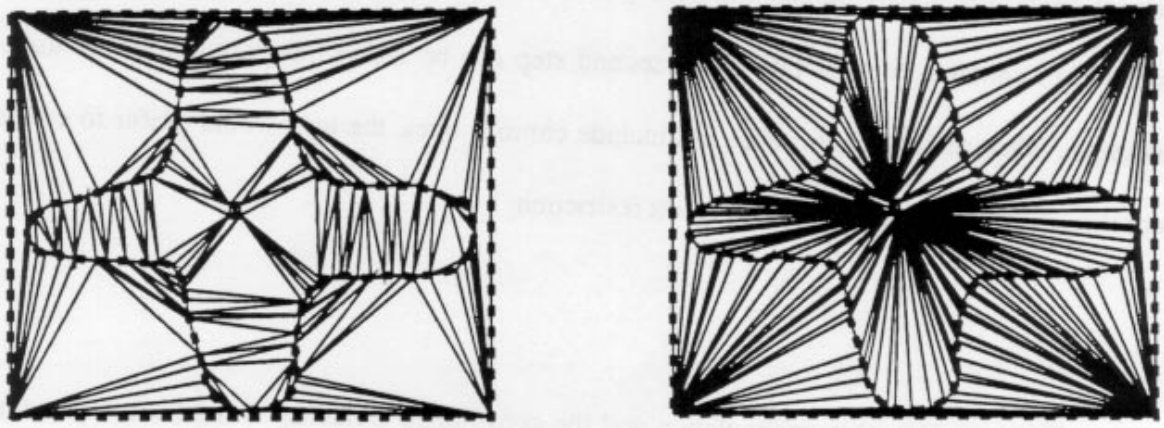

(a) (b)

Figure 5. Triangulations of a simple set of 3 constrained lines
(a) Delaunay triangulation and (b) constrained Delaunay triangulation.

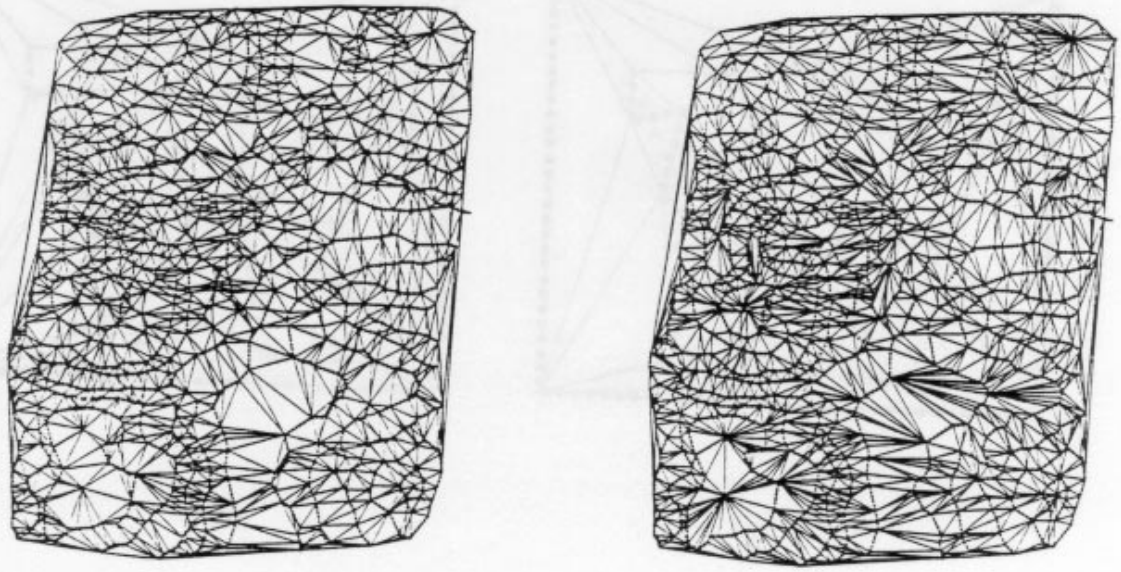

(a) (b)

Figure 6. Triangulations of a complex constrained sample set
(a) Delaunay triangulation and (b) constrained Delaunay triangulation

Figure 4 shows the Delaunay and the constrained Delaunay triangulations of a simple set of 4 constrained lines. In the figure 4(a) the triangles marked with letters A are examples where the Delaunay triangulation crosses constrained segments. The triangles marked with letter B, in the same figure, are examples of undesirable flat triangles when the constrained lines are contour lines. The triangulation pictured in figure 4(b) is the constrained Delaunay triangulation of the same sample set used on the figure 4(a).

Figure 5 shows the Delaunay and the constrained Delaunay triangulations of another simple set of 3 contour lines. In this example we can observe, in figure 5(a), too many flat triangles created by the pure Delaunay triangulation. These flat triangles are avoided when we use the constrained Delaunay triangulation as showed in figure 5(b).

Figure 6 depicts the Delaunay and the constrained Delaunay triangulations of a more complex set of constrained lines.

An analysis of the results presented on figures 4, 5 and 6 can led us to the following question: Are the constrained Delaunay triangulations more representative than the pure Delaunay triangulation? In order to answer this question we can consider two different applications, the extraction of a *contour map* and the derivation of a *slope map*, that can be performed using the triangulations pictured in this section.

Contour map: Suppose that we want to recover the same contour lines that we use as samples in the figures 4, 5 and 6, using only the triangulations pictured in those figures. Although an algorithm to extract contour lines from a TIN was not implemented, it seems to be obvious that one can get more accurate lines from the triangulations of figures 4(b), 5(b) and 6(b) than from those triangulations pictured in figures 4(a), 5(a) and 6(a). An algorithm that recovers the

contour lines should decide what path, immediately above or immediately below, must be followed when a flat area is searched. In addition, on areas where the constrained lines were crossed, the resulting contour lines can be quite different from the original sample.

Slope map: Suppose that the lines presented in the figure 4 are contour lines with different z values associated to them. If we consider a linear surface fitting for each triangle of the triangulation, the regions inside the triangles marked with letter A in the figure 4(a) are examples of areas with slope equal to zero. A visual analysis of that figure shows us that those regions have slopes different from zero and this is better represented in figure 4(b).

6. Conclusions

Although the comparative analysis was only qualitative, the constrained Delaunay triangulation presented in this work seems to be an interesting alternative to take advantage of the properties of the Delaunay triangulation while keeping the final triangulation consistent with the constrained information stored in the input sample set.

When compared to the pure Delaunay triangulation, the constrained Delaunay triangulation requires more computer memory, because of the more complex data structures, and is more time consuming, since it is a two step algorithm. This result was expected and is the price to be paid to have a better result in the final triangulation model. The memory increment is easy to evaluate. The time overhead will be evaluated in future research.

Although the triangulation implemented is a two step algorithm, it avoids complex global analysis each time we have to decide if a sample can be connected to another to create an edge of a new triangle in the triangulation.

Future research in the subject of this work involves a quantitative evaluation of the improvement provided by the constrained Delaunay triangulation described in this work. This must be accomplished by using constrained lines and samples from real surfaces or from mathematically defined functions.

References

AKIMA H., 1978, A method of bivariate interpolation and smooth surface fitting for irregularly distributed data points. *ACM Transactions on Mathematical Software*, 4, 148-159.

BURROUGH, P. A., 1986, *Principles of Geographical Information Systems for Land Resources Assessment* (Oxford: Clarendon Press).

CHEN, Z. -T. and Guevara, J. A., 1987, Systematic selection of very important points (VIP) from digital terrain model for constructing triangular irregular networks. *Proceedings of AUTO-CARTO 8*, Baltimore, MO, U.S.A., pp. 50-56.

DE FLORIANI L. and PUPPO E., 1992, An on-line algorithm for constrained Delaunay triangulation. *CVGIP: Graphical Models and Image Processing*, 54, 290-300.

FALCIDIENO B. and PIENOVI C., 1990, Natural surface approximation by constrained stochastic interpolation. *Computer Aided Design,*, 22, 3, 167-172.

KUMLER M. P., 1992, An Intensive comparison of TINs and DEMs. *PhD Dissertation in Geography*. University of California, Santa Barbara, USA.

LANCASTER P. and SALKAUSKAS K., 1986, *Curve and Surface Fitting: An Introduction*. (London: Academic Press).

MCCULLAGH M. J., 1988, Terrain and surface modeling systems: theory and practice. *Photogrammetric Record*, 12, 747-779.

PREPARATA F. P. and SHAMOS M. I., 1988, *Computational Geometry: An Introduction* (New York: Springer-Verlag).

TSAI V. J. D. 1993, Delaunay triangulations in TIN creations: an overview and a linear-time algorithm. *International Journal of Geographical Information Systems*, 7, 501-524.